Cerebral maturation in the early preterm period - A magnetization transfer and diffusion tensor imaging study using voxel-based analysis

Revital Nossin-Manor[1,2], Dallas Card[1], Charles Raybaud[1,3], Margot J Taylor[1,2], and John G Sled[4,5]

[1]*Diagnostic Imaging, The Hospital for Sick Children, Toronto, ON, Canada,* [2]*Neurosciences & Mental Health, Research Institute, The Hospital for Sick Children, Toronto, ON, Canada,* [3]*Medical Imaging, University of Toronto, Toronto, ON, Canada,* [4]*Physiology Experimental Medicine, Research Institute, The Hospital for Sick Children, Toronto, ON, Canada,* [5]*Medical Biophysics, University of Toronto, Toronto, ON, Canada*

Introduction:

In previous studies we demonstrated the use of magnetization transfer (MT) and diffusion tensor imaging to create group-wise average parametric maps characterizing tissue microstructure of the neonatal brain in very preterm infants (24-32 gestational weeks) scanned at preterm and term equivalent age[1-2]. We showed these parametric maps present distinct contrasts whose interrelations vary across brain regions and between the preterm and term period corresponding to distinct aspects of brain maturation such as tissue organization and myelination. Here we use voxel-based linear regression with age as a covariate to show spatio-temporal variations in cerebral maturation over the whole brain.

Methods:

Subjects: The cohort included 18 preterm neonates born between 27 to 31 gestational weeks (mean±SD, 29.4±1.2 weeks) and scanned within 2 weeks between 28 to 32 weeks (mean±SD, 30.8 ± 1.4 weeks). Informed, written consent was given by the infants' parents; the study was approved by the hospital's research ethics board. Infants presented with normal findings (n=17, including 1 with non-specific minor globus palladi T_1 hyperintensity), and Grade II intraventricular haemorrhage only (n=1) with no extension to the parenchyma.

MR Acquisition: MR scans were performed on a 1.5T GE Signa Excite HD scanner (GE, Milwaukee, WI) using an MR-compatible incubator and neonatal head coil (AIR Inc., Cleveland, OH). High resolution (1x1x1) T_1- and T_2-weighted volumes were acquired using a previously published protocol[3]. MT images were obtained with 1x1x1.5mm voxel size and TR/TE/FA=27ms/4ms/10° by acquiring the sequence once with an off-resonance MT saturation pulse and once without[4]. Twice refocused spin-echo-planar diffusion tensor imaging (DTI) was acquired with 3 non-diffusion and 15 non-collinear diffusion weighted volumes and b=700 s/mm^2 using 1.6mm cubic voxels and TR/TE=15s/85ms[5]. Total scan time for these sequences was 30 min.
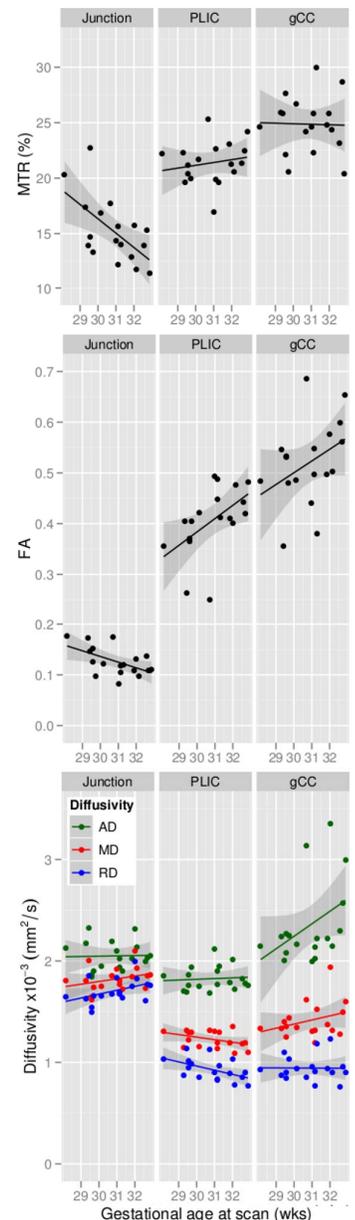
Image Processing: Volume registration and segmentation were done using previously published protocols[1-2,6]. Magnetization transfer ratio (MTR) images were obtained by computing the percent difference between scans with and without the off-resonance pulse. DTI data were processed using the DROP-R algorithm[5] and fractional anisotropy (FA) and mean, axial and radial diffusivity (MD, AD and RD) maps were produced. Group-wise non-linear registration was used to determine anatomical correspondence between individual scans and the average structural / parametric data[2]. A threshold of >50% representation across subjects was applied to the segmented averaged gray matter (GM) and white matter (WM) volumes to construct the corresponding masks.

Analysis: Voxel-based regressions of the above parametric values against age at scan across subjects were calculated to produce volumetric maps of the regression coefficient. At each voxel these analyses included only the subset of subjects where the tissue classification (GM or WM) matched the classification of the group average masks. False discovery rate of 20% was used to threshold regression coefficient maps using R code.

Results& Discussion:

Following the temporal variations in cerebral maturation over the very preterm brain, patches of significant regression coefficient values (q≤0.2) were found in various regions. Different trends of linear evolution of MTR and DTI parameters were observed (Fig.1). These trends, along with the relative values of the quantitative MRI indices, reflect distinct maturational events taking place in the pre-myelinating and early myelinating tissue. For example, the anterior caps and the junction between the genu of the corpus callosum (gCC) and the anterior corona radiate (ACR) in the frontal WM showed relatively low MTR and FA values, indicating low axonal density and tissue directionality, respectively. At the same time, the decrease in MTR and FA values with age, with the decrease in FA (and the increase in MD) driven primarily by an increase in RD, correspond to the migration of radial glial cells towards the frontal cortex at the early preterm stage resulting in a temporary decrease in tissue density in parallel to the reduction in total water content in the frontal WM, axonal formation and increases in crossing fibers. For comparison, while showing similar MTR and FA values, the frontal subplate zone showed a trend of slow decrease in MTR with age with no change in FA, corroborating reduction in cell density and no change in tissue directionality. The gCC demonstrated a different maturational stage, namely, axonal organization, by showing high MTR, FA and AD values along with low RD. Furthermore, gCC showed no change in MTR values with age along with a large increase in FA and AD. On the other hand, the posterior limb of internal capsule (PLIC), a pre-myelinating structure, showed lower values of MTR, FA and AD compared to the gCC, while showing an increase in MTR and FA values with age, no apparent change in AD values and a decrease in MD and RD, corresponding to myelination gliosis and the accumulation of immature oligodendrocytes. These findings elucidate distinct developmental processes in the very preterm brain.

Fig. 1: MTR and DTI parameters vs. age at scan for voxels found significant (q≤0.2) at the junction between the gCC and ACR, PLIC and gCC.

References: 1. Nossin-Manor R et al., 2011. ISMRM 19:2488. **2.** Nossin-Manor R et al., 2013. NeuroImage 64:505–516. **3.** Nossin-Manor R et al., 2011. Pediatr Radiol 41:702-710. **4.** Nossin-Manor R et al., 2012. Radiology 263:510-517. **5.** Morris D et al., 2011. Magn Reson Med 66:92-101. **6.** Card D et al., 2011. ISMRM 19:4321.